Consolidation of Sensitive Clays

Consolidation des Argiles Sensibles

H.B POOROOSHASB — Department of Civil Engineering, Concordia University, Montreal, Quebec
K.T. LAW — Geotechnical Section, Division of Building Research, National Research Council of Canada, Ottawa, Ontario
M. BOZOZUK
W.J. EDEN

SYNOPSIS The mode of deformation of a sensitive clay subjected to stress levels higher than the critical stress is described mathematically. At stress levels above the critical stress, now called overstress, the rate of clay deformation is directly proportional to the magnitude of overstress and the instantaneous value of void ratio. Experimental work, by means of a modified consolidation cell, is described that demonstrates the validity of the postulated model, and indicates how the required parameters are derived.

INTRODUCTION

Long-term case records of the settlement of sensitive clay have revealed that excess pore water pressure in the middle of the compressible layer exists over long periods of time. For example, after 22 years the excess pore water pressure at the Väsby site in Sweden was still equal to the applied vertical pressure (Chang et al. 1973). This was attributed to the generation of pore water pressures due to the collapse of clay structure as consolidation proceeds. Crawford and Burn (1976) report a similar situation in the case of a lightly loaded structure on Leda clay near Ottawa after a period of nearly 20 years. Again these authors suggest that pore water pressures are generated by the collapsing clay structure at a rate equivalent to their dissipation by drainage and result in substantial compression under constant effective stress conditions. Both cited references indicate that separation of the consolidation process into so-called primary and secondary phases is not valid for highly structured or sensitive clays.

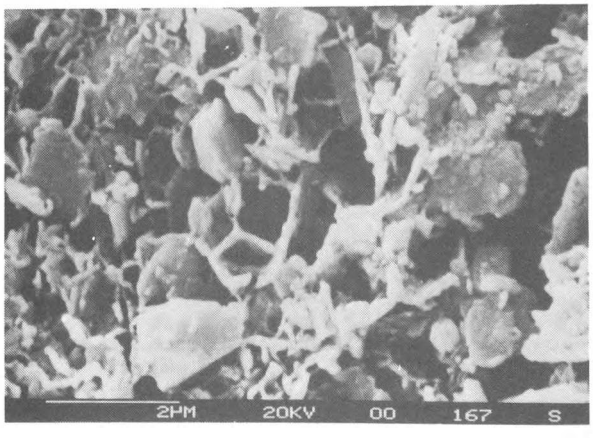

Fig. 1 S.E.M. Photograph of Clay Structure of Kars Clay (After Gillott 1980)

With the advent of the scanning electron microscope, it has been possible to obtain photographs of clay structure and such photographs do indeed confirm the existence of a "card house" or "honeycomb" structure. Figure 1 is a S.E.M. photograph of sensitive clay from the Kars site (Eden and Poorooshasb, 1968). The photograph was taken by Gillott (1980) on a sample supplied by the authors.

With the clay structure and long-term observations as background, a mathematical model, which combines both primary and secondary consolidation with the principle of conservation of mass, a governing equation was derived and solved for various initial and boundary conditions in the form of $S = S\,(T, Z, \frac{\alpha}{aH^2S_o})$, where Z and T are dimensionless space and time variables and α and a are parameters derived from consolidation tests, S_o is a measure of applied stress.

Theoretical Analysis

Denoting the rate of change of voids ratio e by $\dot{e}$ and the effective overstress by $\bar{\sigma}$ where $\bar{\sigma} = \sigma' - \sigma_b$, σ_b being the critical stress and σ' the effective applied stress the constitutive relationship may be expressed in the form

$$\dot{e} = -a\,[e - e_o + \lambda\,\bar{\sigma}]\,\langle\bar{\sigma}\rangle \qquad (1)$$

Constant a is a proportionality coefficient, e_o and λ are soil constants the physical meaning of which may be deduced from Fig. 2. The singularity bracket of equation (1) indicates that for negative values of $\bar{\sigma}$ (σ' smaller than critical stress) the clay is assumed to behave as a rigid material.

From the law of conservation of mass it follows that

$$\frac{\partial e}{\partial t} = -\alpha\,\frac{\partial^2\bar{\sigma}}{\partial z^2} = \alpha\,\frac{\partial^2 u}{\partial z^2} \qquad (2)$$

since $\bar{\sigma} = \sigma_f - u - \sigma_b$ and σ_f and σ_b are assumed constants σ_f being the applied vertical pressure. Coefficient $\alpha = (1 + e)\, k/\gamma_w$ is assumed to remain constant during the loading process.

Let $\lambda\bar{\sigma}$ be denoted by S, and the space and time variables be $Z = z/H$ and $T = \alpha t/\lambda H^2$ where H is the half thickness of the layer with double drainage. Then it can be shown that equation (1) reduces to

$$\frac{\partial e}{\partial T} = - \frac{aH^2}{\alpha} [e - e_o + S]\, S \qquad (3)$$

and equation (2) to

$$\frac{\partial e}{\partial T} = - \frac{\partial^2 S}{\partial Z^2} \qquad (4)$$

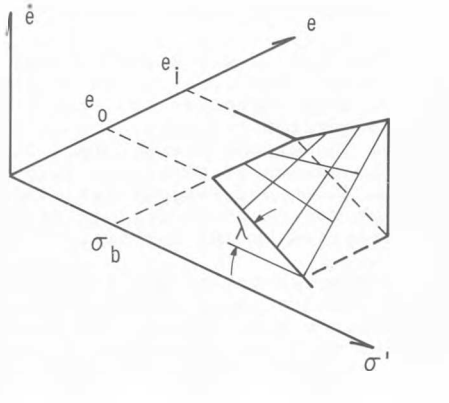

Fig. 2 Model used in Study

Differentiating both sides of equations (3) and (4) with respect to time variable T and equating the results:

$$\frac{\partial^3 S}{\partial T \partial Z^2} = \frac{aH^2}{\alpha} [(\frac{\partial e}{\partial T} + \frac{\partial S}{\partial T})S + (e - e_o + S) \frac{\partial S}{\partial T}] \qquad (5)$$

But from equation (4), $\frac{\partial e}{\partial T} = - \frac{\partial^2 S}{\partial Z^2}$ and from the combination of (3) and (4) $- \frac{\alpha H^2}{\alpha} [e - e_o + S] = \frac{1}{S} \frac{\partial e}{\partial T} = - \frac{1}{S} \frac{\partial^2 S}{\partial Z^2}$. Therefore, equation (5) reduces to

$$+ \frac{\partial^3 S}{\partial T \partial Z^2} = + \frac{aH^2}{\alpha} [\frac{\partial S}{\partial T} - \frac{\partial^2 S}{\partial Z^2}]\, S + \frac{1}{S} \frac{\partial^2 S}{\partial Z^2} \cdot \frac{\partial S}{\partial T} \qquad (6)$$

$$\text{or } [\frac{\partial S}{\partial T} - \frac{\partial^2 S}{\partial Z^2}] = \frac{\alpha}{aH^2 S} [\frac{\partial^3 S}{\partial T \partial Z^2} - \frac{1}{S} \frac{\partial^2 S}{\partial Z^2} \cdot \frac{\partial S}{\partial T}] \qquad (7)$$

Note that if coefficient a is very large i.e. tends to infinity, then the right hand side of equation (7) tends to zero and the theory is identical with the linear theory of Terzaghi-Frölich.

To unify the stress conditions at the boundary let a new variable be defined as $\bar{S}$ where

$$\bar{S} = S/S_F$$

where $S_F = \lambda (\sigma_F - \sigma_b)$, σ_F being the constant pressure applied as defined above. Then equation (7) reduces to

$$[\frac{\partial \bar{S}}{\partial T} - \frac{\partial^2 \bar{S}}{\partial Z^2}] = \frac{\alpha}{aH^2 S_F} [\frac{\partial^3 \bar{S}}{\partial T \partial Z^2} - \frac{1}{\bar{S}} \cdot \frac{\partial^2 \bar{S}}{\partial Z^2} \cdot \frac{\partial \bar{S}}{\partial T}] \qquad (8)$$

which must be solved with the appropriate initial and boundary conditions. In the particular case of constant applied stress these are; at $Z = 1$; $T \geq 0^+$, $\bar{S} = 1$ and at $Z = 0$; $T \geq 0^+$, $\partial\bar{S}/\partial Z = 0$. A detailed discussion of the solution to equation (8) is outside the space limitation of the present paper. (For a detailed account see Poorooshasb and Sivapatham (1969)). It is merely stated that a solution in the form

$$\bar{S} = \bar{S} [Z, T, \frac{\alpha}{aH^2 S_F}] \qquad (9)$$

exists. Preliminary studies by Namachchivaya (1980) has shown that for field conditions (H in excess of a few feet) the dependence of $\bar{S}$ on the parameter α/aH^2S_F is to a first degree of approximation, negligible. Thus it is possible to express $\bar{S}$ as a function of Z and T only under the field conditions. Figure 3 shows the variation of $\bar{S}$ with Z and T. The shape of the isochrones is of particular interest in this figure.

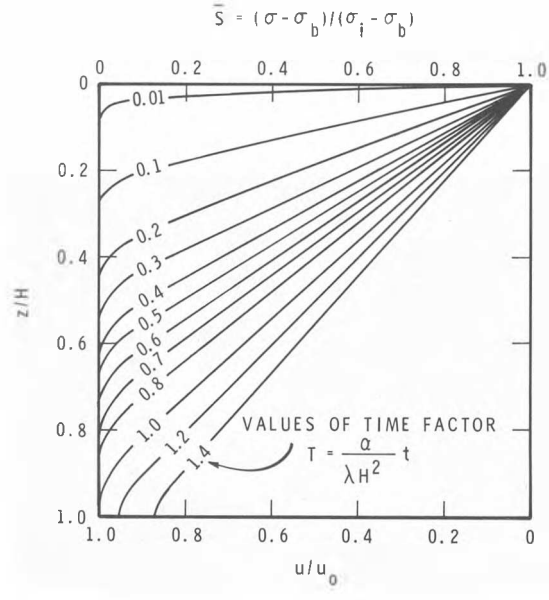

Fig. 3 Consolidation Ratio $\bar{S}$ as a Function at Depth and Time

It is seen that at a time factor of about 1 the midpoint of the layer is still experiencing a substantial pore water pressure, while according to the linear theory this pore water pressure should have dissipated. This is in agreement with observations made in the field. In Fig. 4, the percentage compression of the layer denoted by the ratio of $\delta(T)$, compression at time T to $\delta(T_\infty)$, the final compression of the layer, is plotted as a function of time variable $\sqrt{T}$.

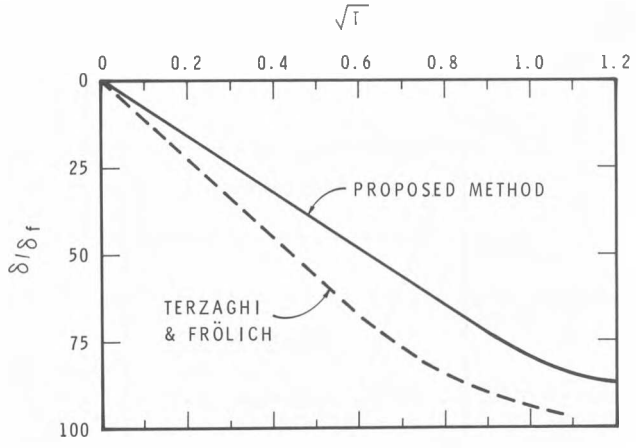

Fig. 4 Compression Ratio Versus Square Root of Time Factor

It is seen that the present theory predicts a considerably longer period for a given percentage of compression than does the linear theory. It is also noted that for the percentage compression values smaller than 75%, or $\sqrt{T}$ less than 0.93, the curve is linear and given by the simple expression

$$\delta(T)/\delta(T_\infty) = 0.8\ T^{1/2} \qquad (10)$$

Tests required to obtain the various parameters used in the theory and the procedure followed for evaluating them are described.

Laboratory Determination of Parameters

To determine the five coefficients employed in the mathematical model, two different consolidation tests have to be conducted in the laboratory. The first involves an incremental loading procedure. During each load increment, the dissipation of excess pore water pressure is observed and the deformation is recorded for a sufficient length of time beyond the end of the dissipation for studying compression under a constant effective pressure. The second test requires loading at a constant strain rate. Any practical strain rate can be used but it is preferable to choose one that will not cause a significant amount of excess pore pressure, because of the resulting simplicity in interpreting the average effective stress.

The apparatus for conducting the two tests is shown in Fig. 5. It is essentially a floating ring device with facilities for application of a back pressure and at the same time for measuring the excess pore pressure. A vertical load is

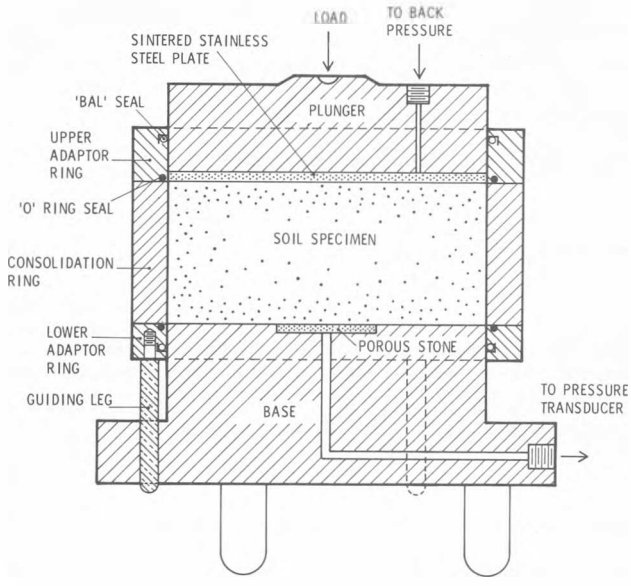

Fig. 5 Consolidation Apparatus used in Study

applied to the soil specimen by means of the plunger. The specimen is consolidated against a back pressure applied through a valve at the top of the plunger. The excess pore water pressure is measured at the base using a pressure transducer which can be detached during mounting of the specimen under water to ensure full saturation in the apparatus. Low friction, teflon-made BAL seals are provided at the adaptor rings. These rings are removed during trimming of the specimen and are replaced by a sharp cutting ring at the top of the consolidation ring. (The consolidation ring is 50.8 mm high and 114.3 mm in diameter.) Three vertical legs, spaced at 120°, and fixed to the lower adaptor rings pass through three stainless steel linear motion bearings. They prevent tilting of the consolidation ring as it moves downwards during compression of the specimen. For the incremental loading test, the apparatus is placed in a loading frame where dead weights are applied. For the constant strain rate test, the apparatus is put in a triaxial load press and the specimen is strained at any selected rate.

The ratio α/λ can be determined from the incremental load test by plotting the compression against the square root of time, $\sqrt{t}$. The resulting relationship, according to Fig. 4, starts to depart from a straight line at $\sqrt{T} = 0.93$. This point is identified on the plot and the corresponding $\sqrt{t}$ value is noted. α/λ can then be evaluated from

$$\sqrt{T} = \sqrt{\left[\frac{\alpha}{\lambda}\right]\frac{t}{h^2}} = 0.93$$

or

$$\frac{\alpha}{\lambda} = 0.865\ h^2/t \qquad (11)$$

where h is the thickness of the soil specimen.

Four more independent equations are required to yield the five coefficients used in the model. To do so, it is easier to consider strain ϵ instead of the change of void ratio, Δe, using the following:

$$\Delta e = -\epsilon\ (1 + e_i) \tag{12}$$

where e_i = initial void ratio.

The basic equation can be rewritten as

$$\dot{\epsilon} = a\ \bar{\sigma}\ [K_1 - \epsilon + K_2\ \bar{\sigma}] \tag{13}$$

where $K_1 = (e_i - e_o)/(1 + e_i)$ (14)

$$K_2 = \lambda/(1 + e_i) \tag{15}$$

For the incremental load test the effective stress is σ_f after excess pore pressure is completely dissipated and a plot of $\dot{\epsilon}$ vs ϵ will yield a straight line with slope m_1

$$m_1 = -a\bar{\sigma} \tag{16}$$

and $$\bar{\sigma} = (\sigma_f - \sigma_b) \tag{17}$$

The intercept of the straight line, b, is given by

$$b = a\bar{\sigma}\ [K_1 + K_2\ \bar{\sigma}] \tag{18}$$

From the test at constant rate of strain, a plot of t vs σ can be obtained. As the strain rate is constant, the slope of the ϵ - σ' curve is given by

$$\frac{\partial \epsilon}{\partial \sigma'} = \frac{\dot{\epsilon}}{a\bar{\sigma}^2} + K_2 \tag{19}$$

At large $\bar{\sigma}^2$, $\frac{\partial \epsilon}{\partial \sigma'} = K_2$ (20)

Let m_3 be the slope of ϵ-σ' curve at the same effective stress as in equation (16), then

$$m_3 = \frac{\dot{\epsilon}}{a\bar{\sigma}^2} + K_2 \tag{21}$$

λ can be obtained directly from equation (15),

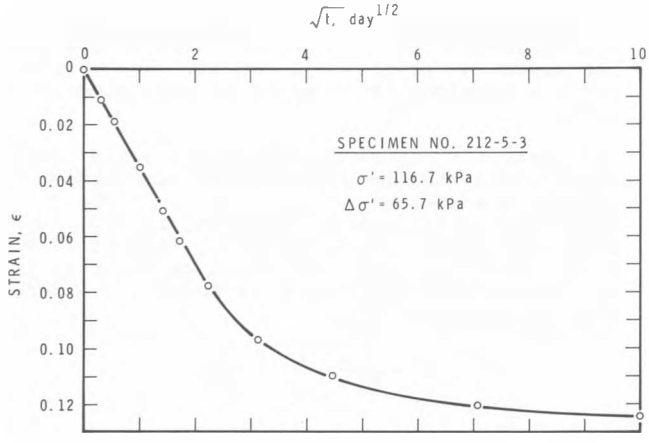

Fig. 6 Results of Incremental Loading Consolidation Test

σ_b by solving equations (16), (17) and (19) simultaneously, a from euqation (16), e_o from equations (18) and (14), and α from equation (11).

To illustrate, tests were conducted on samples of soft marine clay with moisture content of 68%, plastic limit of 20%, liquid limit of 55% and e_i = 2.32. Figure 6 shows a ϵ - $\sqrt{t}$ plot at σ' = 116.7 kPa which exceeds the bonding stress σ_b. The compression departs from the linear relationship at $\sqrt{t}$ = 2.75 day$^{1/2}$ which corresponds to the 75% consolidation predicted in the theory. Hence from equation (11) α/λ = 2.95 cm^2/day.

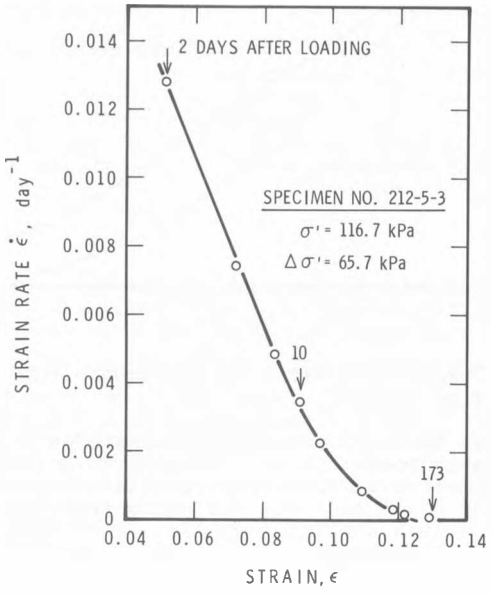

Fig. 7 Strain Rate vs Strain for Incremental Loading Consolidation Test

Figure 7 shows the plot of $\dot{\epsilon}$ vs ϵ. Within the range of practical interest, a straight line relationship is obtained, yielding

$$m_1 = -0.247/\text{day};$$

and $$b = 0.025/\text{day}.$$

Figure 8 shows the stress-strain relationship for the clay conducted at a constant strain rate of 0.015/day. The slopes at σ' = 116.7 kPa and at large σ' are 0.001215/kPa and 0.000326 kPa, respectively. From these numbers, the following are obtained for the coefficients:

σ_b = 48 kPa

a = 0.0036/kPa/day

λ = 0.00108/kPa

e_o = 2.06

α = 2731 cm^2/kPa/day

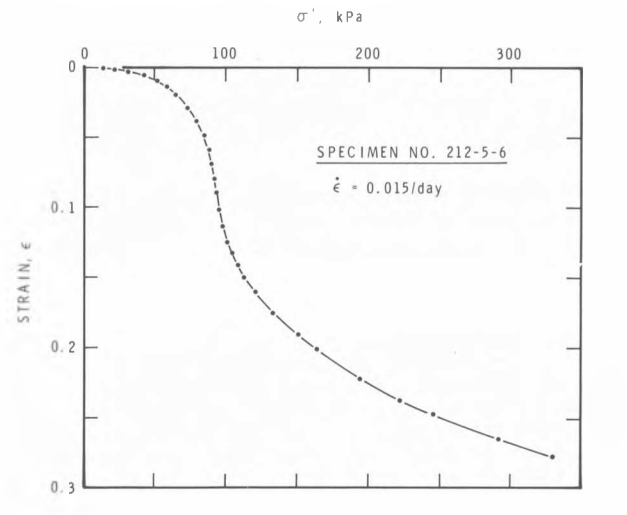

Fig. 8 Results of Constant Strain Rate Consolidation Test

Discussion

A model has been presented which adequately describes the consolidation behaviour of undisturbed samples of sensitive clay in the laboratory. In the initial stages of consolidation, the percentage consolidation depends linearly on the square root of time up to about 75% of the total deformation, at a much slower rate than predicted by the linear theory of Terzaghi. The model correctly describes the strain rate effects observed by Crawford (1964) and Jarrett (1967).

At the present time, too few laboratory test results are available to attempt a detailed comparison with a field record of settlement of a full-scale load. The paper shows how the parameters are obtained from modified laboratory tests and through the use of the curves given in Fig. 3 and 4, field settlements of clay layers may be calculated.

Acknowledgements

The authors wish to thank Dr. J.E. Gillott of the University of Calgary for the use of the S.E.M. photograph used in Fig. 1. The paper is a joint contribution of the Department of Civil Engineering, Concordia University, Montreal, and the Division of Building Research, National Research Council of Canada. It is published with the approval of the Director of the Division of Building Research.

References Cited

Chang, Y.C.E., Broms, B. and Peck, R.B. (1973). Relationship between the settlement of soft clays and excess pore pressure due to imposed loads. Proc. 8th ICSMFE, Moscow, Vol. 1:1, pp. 93-96.

Crawford, C.B. (1964). Interpretation of the consolidation test. Proc. A.S.C.E., Journal S.M.F.D., Vol. 90, No. SM5, pp. 87-102.

Crawford, C.B. and Burn, K.N. (1976). Long-term settlements on sensitive clay. Laurits Bjerrum Memorial Volume, pp. 117-124, Norwegian Geotechnical Institute, Oslo.

Eden, W.J. and Poorooshasb, H.B. (1968). Settlement observations at Kars bridge. Canadian Geotechnical Journal, Vol. 5, No. 1, pp. 29-46.

Gillott, J.E. (1980). Use of the scanning el electron microscope and fourier methods in characterization of microfabric and texture of sediments. Journal of Microscopy (In Press).

Jarrett, P.M. (1967). Time-dependent consolidation of a sensitive clay, Vol. 7, No. 7, pp. 300-304.

Namachchiraya, N. Sri, (1980). Consolidation of sensitive clays-(1980). Thesis to be submitted to the University of Waterloo, in partial fulfillment of requirements for the M.Sc. degree.

Poorooshasb, H.B. and Sivapatham (1969). Consolidation of sensitive clays exhibiting strong structural breakdown, Seventh Internal Conference on Soil Mechanics and Foundation Engineering, Mexico City, Mexico. Proceedings of Specialty Session No. 12, pp. 27-37.